

OutFlank Routing: Increasing Throughput in Toroidal Interconnection Networks*

Francesco Versaci

Vienna University of Technology

Abstract

We present a new, deadlock-free, routing scheme for toroidal interconnection networks, called OutFlank Routing (OFR). OFR is an adaptive strategy which exploits non-minimal links, both in the source and in the destination nodes. When minimal links are congested, OFR deroutes packets to carefully chosen intermediate destinations, in order to obtain travel paths which are only an additive constant longer than the shortest ones. Since routing performance is very sensitive to changes in the traffic model or in the router parameters, an accurate discrete-event simulator of the toroidal network has been developed to empirically validate OFR, by comparing it against other relevant routing strategies, over a range of typical real-world traffic patterns. On the $16 \times 16 \times 16$ (4096 nodes) simulated network OFR exhibits improvements of the maximum sustained throughput between 14% and 114%, with respect to Adaptive Bubble Routing.

Keywords: Routing, Interconnection networks, Adaptive routing, Toroidal networks, High performance computing.

1 Introduction

Tori are key topologies for the interconnection networks of parallel computers, both in multiprocessors machines and on-chip multiprocessors [17]. E.g., the Fujitsu K computer features a six-dimensional torus network [3], IBM BlueGene/Q a five-dimensional one [13], while both the Cray XT series [11] and IBM BlueGene/L and P [2, 4] have a three-dimensional one. Furthermore, the adoption of mesh-like topologies is bound to increase even more, since they represent the only scalable solution under a limiting technology point of view [8].

Routing is the fundamental problem of choosing paths (or other network resources, such as link queues) for packets which travel in a network, between a source node s and a destination node t , and has been studied intensively, both by theoretical means and empirical investigations. Typically, routing is studied under some permutation pattern, which causes each node to send and receive the same amount of data. Routing algorithms can be roughly classified in *oblivious*, for which the path from s to t depends only on s and t (and optionally on some randomness), and *adaptive*, for which decisions on the path can also

depend on online network parameters, such as, e.g., congestion at edges.

Theoretical investigations have primarily focused on oblivious algorithms, partly because of the difficulties encountered in analyzing adaptive ones, exemplified in 1982 by L. Valiant [37]: “Unfortunately such [adaptive] strategies appear to be beyond rigorous analysis or testability”. The first nontrivial lower bounds concerning a wide class of adaptive algorithms for the two-dimensional mesh have been presented in [7, 14] (and, furthermore, are the first to take into account bounded queues in the routers). Among oblivious strategies there is a large performance gap if randomness is allowed: e.g., deterministic policies perform far from optimal under a worst-case congestion metrics, since on a graph with N nodes and maximum degree d there always exists a permutation which causes edge congestion $\Omega(\sqrt{N}/d)$ [10, 23] while, on the other hand, randomized strategies can achieve a $O(\log N)$ competitive ratio against the optimal offline [12, 29, 30, 38, 40]. However, in current supercomputers randomized oblivious strategies have seldom been implemented, a notable exception being the recent PERCS interconnect [6].

Though difficult to analyze, adaptive routing algorithms have shown to perform remarkably well on real machines and have thus been adopted, e.g., by IBM BlueGene/L, P and Q [4, 9, 13], Cray T3E [32] and Quadrics [22]. An important property of adaptive algorithms is whether they are *minimal*, i.e., if they allow only shortest paths from source to destination (if *any* shortest path is admissible then they are called *fully minimal*). Minimal strategies ensure shortest delivery time when the network is under-loaded and preclude *livelock*, i.e., the possibility for a packet to move indefinitely in the network without reaching its destination. On the other hand, minimal strategies underutilize the network bandwidth: e.g., on a three-dimensional torus there are six outgoing links from each node, but only three (or less) of these lie along minimal directions to a given destination node; hence, the maximum throughput achievable in the torus by a minimal routing can be half (or less) of the one achievable by allowing non minimal paths.

An interesting technique for increasing the maximum throughput while keeping the router complexity low has been proposed by Singh et al. [33–36] for k -ary n -cubes (i.e., for n -dimensional tori with length k in each dimension). They have suggested to deroute packets non-minimally along “crowded” dimensions, in order to decrease the congestion of the *minimal orthant*, i.e., the part of the network which contains all (and only) the minimal paths. In more detail, to route each *newly*

*To appear in the 19th IEEE International Conference on Parallel and Distributed Systems (ICPADS 2013).

injected packet, the router can choose among 2^n orthants, based on the congestion of the outgoing links. Once the orthant has been decided (e.g., $(x+, y-)$ in two dimensions), the packet can travel in each dimension only according to the associated directions. In the following, we refer to such a general strategy (which comprises the GAL, GOAL and CQR policies) as Pick Orthant Routing (POR). This kind of derouting has the clear advantage of spreading the traffic along the network, hence decreasing the congestion in hot spots, but can arbitrarily lengthen a path, since it may force a packet, which has as destination a neighbor of the source node, to move in the non-minimal direction all around the torus (thus traversing $k - 1$ nodes instead of just one).

In this work, we propose an adaptive strategy which tries to make use of the full bandwidth while also limiting the path dilation to an *additive constant*. The OutFlank Routing (OFR) schematically works as follows: when the minimal links are congested it starts derouting packets to Intermediate Destination Nodes (IDNs). There are two types of IDNs which are considered: Wraparound IDNs, which mimic the POR routing strategy, and OutFlank IDNs, which *outflank* the minimal orthant and only increase the path length by a constant value, while still exploiting the available non-minimal links, both in the source and the destination nodes (see Fig. 1 for an example in two dimensions). Another interesting feature of the OFR policy comes from the fact that, by using only OutFlank IDNs, it might also be adapted to work on (non-toroidal) mesh networks, whereas the POR strategy is strictly linked to the toroidal topology. In this paper, however, we will consider only toroidal networks, in order to have a more uniform comparison with related routing strategies. Since routing performance is very sensitive to changes in the traffic generation model or in the parameters of the adopted routing strategy, we have developed an accurate discrete-event simulator of the toroidal networks (built on top of the OMNeT++ network simulation framework [39]), which we have used to empirically validate OFR. In detail, we have compared it against both POR and the Adaptive Bubble Router [27, 28] (ABR, described in Sec. 2), adopted in BlueGene machines, for various real-world traffic patterns.

The paper is structured as follows: in Section 2 we present the model adopted for the network and the traffic generation and review some relevant results which will be used later; in Section 3 we illustrate OFR for general toroidal topologies, giving a detailed description of the widespread two and three-dimensional cases; in Section 4 we describe the discrete-event simulator and discuss the experimental results obtained; finally, Section 5 contains the conclusions.

2 Network model and preliminaries

We consider n -dimensional toroidal interconnection networks, with bidirectional links between the nodes. Each physical node comprises of

1. a generator which produces the packets to be sent,
2. a router which routes the packets,

3. a sink which consumes the packets.

Traffic is generated in bunches of M packets, all having the same destination (a bunch represents a *message*), which are injected into the router via a dedicated link with bandwidth B_{int} and latency λ_{int} . A similar link connects the router to the sink. The router has outgoing links to its $2n$ neighbors, with bandwidth B_{ext} and latency λ_{ext} . Typically, the packets size S is chosen to have λ_{ext} and $\frac{S}{B_{\text{ext}}}$ of the same order of magnitude, so that (i) programs which perform small communications do not suffer large latencies due to a large packet size, (ii) programs which communicate with large chunks of data do not suffer too much overhead from fragmentation of the messages.

Switching of packets in routers is generally categorized in:

Store-and-forward: Messages are split in packets and sent *independently*. Each packet is received, stored completely in a router queue and then forwarded.

Wormhole: Messages are divided into flits, which are *orderly* routed along the *same* path [16]. Routers can forward a message if they have storage space for at least one flit.

Virtual cut-through: Messages are split in packets, sent *independently*. Packets are forwarded only if there is enough space to store them completely. As soon as the packet header is read the whole packet is *simultaneously* buffered locally and forwarded to an outgoing link [24].

The OFR paradigm applies to all of the above switching techniques, but the current simulator employed in Sec. 4 implements a store-and-forward approach.

When designing a routing strategy a main concern is to avoid *deadlocks*, i.e., presence of packets permanently stuck because of circular dependencies in the resource requests. The theory of deadlock [15, 16, 18, 19] typically makes use of various virtual channels to increase the available links, so as to be able to impose a priority order in the resources usage and remove the possibility of circular dependencies. A different, simpler approach [31] has been adopted by ABR [27, 28], which works by preventing all buffers to get completely filled: if some free slots (*bubbles*) are always left in the network, then packets can constantly move and deadlock cannot occur. In detail, ABR has two Virtual Channels (VCs) for each unidirectional link, an *escape* (bubble) one and an *adaptive* one. Packets in the escape network move in dimension order and can be injected into a router (from the generator or from a lower dimension) only if there are at least *two* slots available. (The dimension order breaks deadlocks between packets moving along different dimensions, the bubble rule breaks deadlocks inside one-dimensional cycles.) The adaptive subnetwork complements the escape one: packets are preferably routed into adaptive queues, if available; any adaptive queue lying along a minimal path can be chosen (fully minimal) and only when all the adaptive queues are full, escape queues are considered (packets moving from adaptive to escape queues are regarded as injection, i.e., two free slots are required for the insertion).

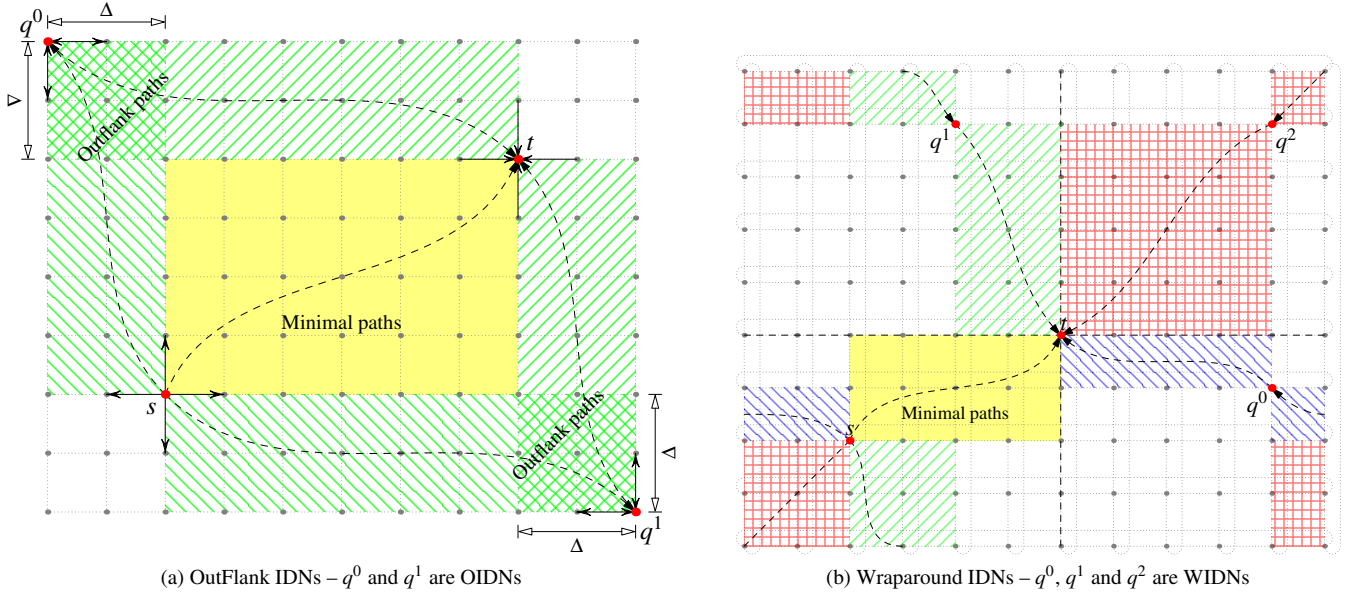


Figure 1: OutFlank routing in the two-dimensional torus.

3 The OFR algorithm

OFR can be regarded as a higher level mechanism which exploits an underlying minimal router: when a packet is firstly injected into the network, OFR decides if it is convenient to deroute it and, if that is the case, chooses a suitable IDN q for it; packet header is extended to include the optional IDN and packets are first routed (*minimally*) to their IDN (if they have one) and then to their final destination. We have chosen to adopt ABR as the underlying minimal routing scheme for OFR. The main task of OFR is to carefully choose if and where to deroute a packet. In this section we thoroughly describe these mechanisms. In §3.1 we define the set of admissible IDNs which can be used for derouting; in §3.2 we see how to adaptively choose among the possible IDNs, weighting congestion and path dilation; in §3.3 we discuss how to prevent deadlock and livelock to occur when using OFR.

3.1 Admissible IDNs

Consider an n -dimensional toroidal network of size $k_1 \times \dots \times k_n$, a source node s with coordinates $s = (s_1, \dots, s_n)$ and a destination node $t = (t_1, \dots, t_n)$. There are $2n$ outgoing links from s and $2n$ incoming links to t , providing an upperbound on the exploitable bandwidth between s and t . Each of the above links can be minimal (μ -link) or non-minimal (ν -link). Each dimension, under the point of view of the source s , $i \in \{1, \dots, n\}$, can be classified either as:

1. $\mu\nu$ (minimal/non-minimal), if $s_i \neq t_i$,
2. $\nu\nu$ (non-minimal/non-minimal), if $s_i = t_i$.

We call \mathcal{M} the set of all $\mu\nu$ dimensions, and \mathcal{N} the set of all $\nu\nu$ dimensions. (If $i \in \mathcal{M}$, then one of the two outgoing links from s along dimension i is a μ -link, and the other one is a ν -link; if $i \in \mathcal{N}$, then both the two outgoing links from s

along dimension i are ν -links.) Minimal routers use only μ -links, both in the source and in the destination nodes, and hence cannot exploit $\nu\nu$ dimensions. OFR strategy takes advantage also of ν -links, both along $\mu\nu$ and $\nu\nu$ dimensions.

OFR exploits non-minimal links by considering two kinds of possible IDNs: Wraparound IDNs (WIDNs) and OutFlank IDNs (OIDNs).

3.1.1 Wraparound IDNs

WIDNs enable OFR to mimic POR behavior. In more detail, let β be an n -dimensional binary vector: $\beta = (\beta_1, \dots, \beta_n) \in \{0, 1\}^n$, then an admissible WIDN $q(\beta) = (q_1(\beta_1), \dots, q_n(\beta_n))$, is defined by setting

$$q_i(\beta_i) = \left\lfloor \frac{s_i + t_i + \beta_i k_i}{2} \right\rfloor. \quad (1)$$

When β varies over all the possible 2^n values, the associated WIDNs lie in the middle of each of the 2^n orthants (including the minimal one, which can be discarded since it would not deroute the packet). By forcing a packet to go through a WIDN we make it wrap around some edges, thus simulating the POR behavior (see Fig. 1b for an example in the two-dimensional case).

3.1.2 OutFlank IDNs

OIDNs are the IDNs which allow OFR to achieve constant dilation by *locally* derouting a packet. Intuitively speaking, the OIDNs are chosen near the vertices of the minimal orthant and outside of it (e.g., Δ steps outside in each dimension). Formally, OIDN $q(\lambda) = (q_1(\lambda_1), \dots, q_n(\lambda_n))$ is determined by choosing

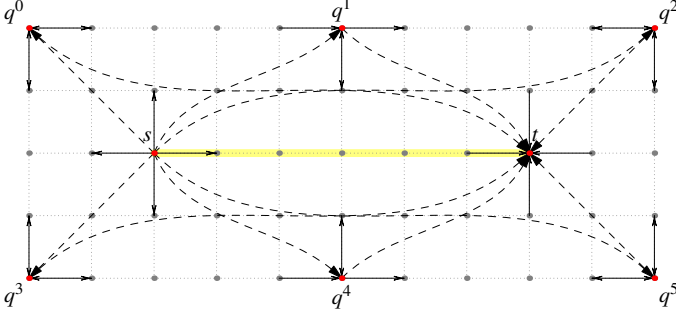


Figure 2: OFR – Admissible OIDNs for collinear s and t (two-dimensional case).

for each dimension i a value $\lambda_i \in \{-1, 0, 1\}$ s.t.

$\forall i \in \mathcal{M}$

$$q_i(\lambda_i) = \begin{cases} (s_i - \Delta) \bmod k_i, & \lambda_i = -1 \wedge i- \text{ is a } \nu\text{-link} \\ (t_i - \Delta) \bmod k_i, & \lambda_i = -1 \wedge i- \text{ is a } \mu\text{-link} \\ (s_i + \Delta) \bmod k_i, & \lambda_i = 1 \wedge i+ \text{ is a } \nu\text{-link} \\ (t_i + \Delta) \bmod k_i, & \lambda_i = 1 \wedge i+ \text{ is a } \mu\text{-link} \\ \lfloor \frac{s_i + t_i}{2} \rfloor, & \lambda_i = 0 \end{cases}, \quad (2)$$

$\forall i \in \mathcal{N}$

$$q_i(\lambda_i) = \begin{cases} s_i + \lambda_i \Delta \bmod k_i, & \lambda_i \in \{-1, 1\} \\ s_i, & \lambda_i = 0 \end{cases}, \quad (3)$$

where Δ is a router parameter ($\Delta = 2$ in the simulations of Sec. 4). Furthermore, OIDNs are chosen so as to exploit at least a ν -link both in s and in t . Let us now see an example of the admissible OIDNs to help clarify the general procedure.

Example 1 (OFR in two-dimensional tori). Consider Fig. 1a: s and t have different coordinates in both the dimensions, so both 1 (i.e., x) and 2 (i.e., y) belong to \mathcal{M} . The minimal orthant is the yellow area, and the μ -links are $(x+, y+)$. Since we want to use both a μ -link and a ν -link, the two possible choices are $(x-, y+)$ and $(x+, y-)$, which correspond to OIDNs q^0 and q^1 and λ values $(1, -1)$ and $(-1, 1)$. Now consider the case, illustrated in Fig. 2 of s and t collinear. In this case $x \in \mathcal{M}$ and $y \in \mathcal{N}$, so the admissible choices for λ are:

$$\lambda^0 = (-1, 1), \quad \lambda^1 = (0, 1), \quad \lambda^2 = (1, 1), \quad (4)$$

$$\lambda^3 = (-1, -1), \quad \lambda^4 = (0, -1), \quad \lambda^5 = (1, -1), \quad (5)$$

which induce the six OIDNs q^0, \dots, q^5 represented in Fig. 2.

Remark 1. When designing the actual router, not all the admissible OIDNs need to be considered for derouting, but it suffices to choose a subset of them which covers all the ν -links, both in the source and destination nodes. E.g., in the case of collinear s and t of Example 1, the four OIDNs q^0, q^2, q^3 , and q^5 are enough for enabling full bandwidth between s and t .

Remark 2. If for some dimension i the distance between s_i and t_i is not smaller than $\frac{k_n}{2} - \Delta$, then the computed OIDNs can “jump” into another orthant because of the torus wraparound.

The above procedure still works correctly, but the OIDNs obtained now behave, for some dimensions, similarly to WIDNs (because of the wraparound).

Outflanking through an OIDN causes a path dilation: the total derouted distance $\tilde{d}(s, t)$ is larger than the minimal distance $d(s, t)$. In detail, using an OIDN q yields an additional path distance $\delta(q)$, but this extra-distance is always bounded by a constant (once n and Δ are fixed):

$$\tilde{d}_q(s, t) := d(s, q) + d(q, t) = d(s, t) + \delta(q), \quad \forall q \delta(q) \leq 2n\Delta. \quad (6)$$

We have set Δ to a constant, but one might also consider to set Δ to be a fraction of $d(s, t)$, so as to increase the outflank throughput while keeping the dilation bounded by a *multiplicative* factor. Focusing again on Fig. 2, the additive dilations of the admissible OIDNs are

$$\delta^0 = 4\Delta, \quad \delta^1 = 2\Delta, \quad \delta^2 = 4\Delta, \quad (7)$$

$$\delta^3 = 4\Delta, \quad \delta^4 = 2\Delta, \quad \delta^5 = 4\Delta. \quad (8)$$

Using the dilations above we can choose another subset of the admissible OIDNs which still covers all the ν -links as before, but induces smaller dilations (e.g.: q^0, q^1, q^4 , and q^5).

Example 2 (OFR in three-dimensional tori). We list now the OIDNs used by the OFR router for the three-dimensional case (the one implemented in the simulator). We assume, w.l.o.g., that if a μ -link exists along some dimension i , then it is positively oriented ($i+$).

- $s_1 \neq t_1, s_2 \neq t_2, s_3 \neq t_3$ (s and t not coplanar)

$$\lambda^0 = (0, -1, 1), \quad \lambda^1 = (0, 1, -1), \quad \lambda^2 = (-1, 0, 1), \quad (9)$$

$$\lambda^3 = (1, 0, -1), \quad \lambda^4 = (-1, 1, 0), \quad \lambda^5 = (1, -1, 0). \quad (10)$$

- $s_1 = t_1, s_2 \neq t_2, s_3 \neq t_3$ (s and t coplanar but not collinear, see Fig. 3)

$$\lambda^0 = (0, -1, 1), \quad \lambda^1 = (0, 1, -1), \quad (11)$$

$$\lambda^2 = (1, 0, 0), \quad \lambda^3 = (-1, 0, 0). \quad (12)$$

- $s_1 = t_1, s_2 = t_2, s_3 \neq t_3$ (s and t collinear)

$$\lambda^0 = (1, 0, 1), \quad \lambda^1 = (-1, 0, 0), \quad (13)$$

$$\lambda^2 = (0, 1, -1), \quad \lambda^3 = (0, -1, 0). \quad (14)$$

3.2 Choosing the IDN

To choose the most rewarding intermediate destination, OFR computes a profit for each available IDN, taking into account both the dilation and the congestion of the alternative route. In more detail, OFR works as follows:

1. When a packet is newly injected, the router computes a set \mathcal{Q} of IDNs that covers all the ν -links from s to t .

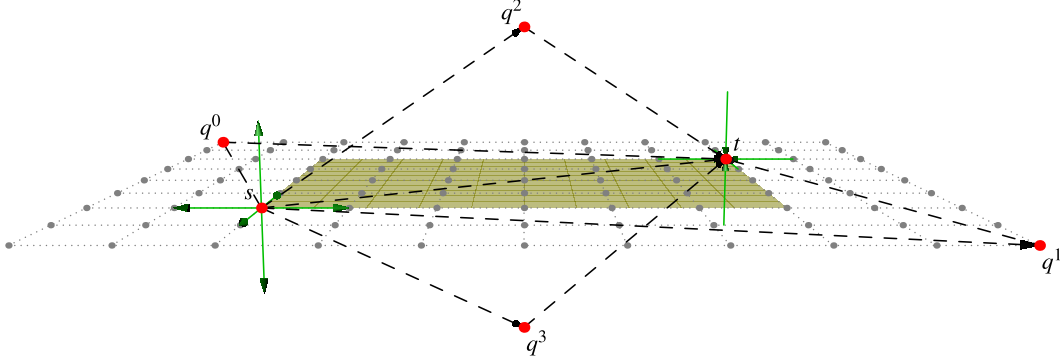


Figure 3: The four OIDNs used by OFR for coplanar s and t (three-dimensional case).

2. For each $q \in \mathcal{Q}$ two values are computed:
 - (a) The total distance $\tilde{d}_q(s, t) = d(s, q) + d(q, t)$.
 - (b) The average number $u_q(s)$ of used (non free) slots in the (local) outgoing links which are minimal from s to q .
3. We obtain a single profit, by scalarizing the two metrics in which we are interested, as

$$\pi_q(s, t) := \frac{u_*(s)}{u_q(s, t)} + \eta \frac{d(s, t)}{\tilde{d}_q(s, t)}, \quad (15)$$

where $u_*(s)$ is the minimum number of used slots in a link going out from s and η is parameter tuned empirically ($\eta = 2.0$ in the simulations of Sec. 4). Also, the first fraction is set to one whenever $u_q(s, t) = u_*(s) = 0$.

4. The analogous profit is computed also for the minimal (not outflanked) routing:

$$\pi_0(s, t) := \frac{u_*(s)}{u_0(s, t)} + \eta, \quad (16)$$

where $u_0(s)$ is the average number of used slots in μ -links from s .

5. If, for all q , $\pi_0(s, t) \geq \pi_q(s, t)$, then the packet is routed minimally and no derouting is performed.
6. Otherwise, q^* is chosen as IDN, such as

$$q^* := \arg \max_q \pi_q(s, t). \quad (17)$$

Remark 3. The same procedure has been used in our simulations to decide when to deroute packets while adopting POR, but the parameter η has been independently optimized ($\eta = 1.0$ for POR).

3.3 Deadlock and livelock

In order to be usable, any routing policy needs to be deadlock-free, or to include some mechanism to detect deadlocks and recover from them [5, 25]. OFR, being a non-minimal strategy, might also be subject to livelocks. Actually, if not carefully implemented, OFR can produce deadlocks: if a packet reaches

an IDN and the router simply tries to reroute it towards its final destination, then a loop of dependencies might arise from other packets, since derouting interferes with ABR dimension order routing in the escape subnetwork.

The following two theorems prove that OFR can be implemented without deadlocks and livelocks.

Theorem 1. *OFR can be implemented in a deadlock-free way by adopting VCs in the escape network.*

Proof. OFR can interfere with ABR mechanisms to prevent deadlocks in the following way: when a packet reaches its intermediate destination and it is rerouted toward its final destination, it might come from an ABR escape VC and try to enter into another escape VC which is lower in the dimension order used by ABR. This could lead to cyclic dependencies and hence deadlock in OFR. To avoid this, it is enough to split the escape subnetwork in two virtual escape subnetworks VS1 and VS2. VS1 is used only by packets which are reaching an IDN, whereas VS2 is used only by packets routed towards their final destination (note that we only need to split the escape subnetwork, not the adaptive one). An insertion into VS2 of a packet which has reached its IDN is treated as an injection, i.e., the insertion is allowed only if it does not saturate the queue. Packets which have entered VS2 will always be delivered, since VS2 is deadlock-free and does not depend on other external resources. Therefore, some resource will be freed up for packets which want to enter in VS2 from VS1 (or directly from the generators if no IDN is given for a packet), propagating the deadlock-freedom to the whole network. \square

Theorem 2. *OFR is livelock-free.*

Proof. OFR deroutes packets by transforming a path $s \rightarrow t$ into a longer path $s \rightarrow q \rightarrow t$. Since derouting can only happen to newly injected packets (i.e., once in a packet lifetime) there cannot be path decompositions with more than one intermediate destination. Since each of the two travel phases $s \rightarrow q$ and $q \rightarrow t$ are routed minimally, livelock cannot occur. \square

4 Experimental validation

Routing performance is extremely sensitive to implementation details, network architecture and algorithmic parameters. To get a realistic estimate of OFR behavior we have therefore

chosen to develop an accurate network simulator. Our discrete event simulator has been written within the OMNeT++ network simulation framework [39]; the simulator code will be released under the GNU Lesser General Public License v3.0 [21]. The implemented network is inspired by the three-dimensional toroidal network being developed within the AuroraScience project [26].

We have tested the network performance of OFR under a sustained traffic and with different communication patterns, and we have compared OFR with both ABR and POR routing schemes. To make the comparison as uniform as possible we have implemented POR (as well as OFR) in an ABR-like fashion and we have chosen when to deroute packets for POR using the technique described in §3.2 for OFR, but optimized independently for maximizing POR performance.

Traffic is generated in bursts (messages) of M packets, according to the chosen communication pattern. The offered load γ , the rate at which packets are generated, is normalized as follows: it is equal to $\gamma_0 = 1$ when it saturates the bisection bandwidth of the network under uniform traffic (i.e., $\gamma_0 = 1$ is an upper bound to the sustainable injection rate if the packets are sent to uniformly random destinations). Depending on the communication pattern P and routing algorithm R there is a value $\gamma^*(R, P)$ at which the network is saturated and cannot sustain the traffic (i.e., the average lifetime of the packets grows to infinity). We are interested in both the maximum sustained throughput γ^* and in the average latency of packets for fixed values of the offered load γ . In the plots of Fig. 4 we show, for each simulated communication pattern on the 16×16 network, the average packet lifetime as a function of γ . The times are plotted only for values of γ which did not saturate the network (i.e., times not reported are infinite). A summary of the achieved maximum throughputs γ^* , for the tested routing algorithms and communication patterns, both for $k = 8$ and $k = 16$, is given in Table 2. The following five communication patterns have been simulated (note that all but the first one are permutation patterns):

Uniform: Destinations are chosen independently and uniformly at random for each message.

Butterfly/FFT: Messages are sent to nodes with Hamming distance one; the position of the flipped bit is increased at each message. This communication pattern is used, e.g., in FFT and bitonic sort.

Transposition: The usual matrix transposition: $(i, j) \mapsto (j, i)$. It assumes the number of nodes N to be square.

3D Transposition: 3D coordinates rotation: $(x, y, z) \mapsto (y, z, x)$ (this communication pattern has applications in medical imaging and 3D-FFT [20]).

Bit-Reverse: Destination is the bit reverse of the source (e.g., 0100 \mapsto 0010). This pattern (which appears, e.g., in the FFT) is the worst case one for Dimension Order Routing on n -dimensional mesh-like networks.

We have simulated three-dimensional toroidal networks, therefore each router is connected to six neighbors. For each unidirectional link there are three VCs (one adaptive and two

Table 1: Parameters of the simulator.

Parameter	Description	Value
S	Packet size	512 B
C	Queues capacity	8 packets
M	Message size	96 packets
λ_{int}	Internal latency	80 ns
B_{int}	Internal bandwidth	64 Gb/s
λ_{ext}	External latency	200 ns
B_{ext}	External bandwidth	20 Gb/s
k	Network size ($k \times k \times k$)	8 or 16

Table 2: maximum throughput γ^* (in γ_0 units) on $k \times k \times k$ networks (except Transposition which has been tested on a $16 \times 8 \times 8$ and on a $16 \times 16 \times 16$ networks). Best results for each pattern/network size k are highlighted in bold.

Pattern	ABR		POR		OFR	
	$k = 8$	16	8	16	8	16
Butterfly/FFT	0.30	0.35	0.55	0.55	0.60	0.75
Transposition	0.50	0.55	0.60	0.70	0.50	0.75
3D Transposition	0.25	0.20	0.45	0.40	0.45	0.35
Uniform	0.55	0.70	0.70	0.80	0.70	0.80
Bit-Reverse	0.35	0.40	0.60	0.50	0.50	0.60

escape ones) and the capacity of each VC is C packets. Routers also handle ACKs/NAKs to acknowledge packets acceptance, but we omit the details in this paper due to space limitations. Available packets are sent to the router for injection at rate $2.4 \gamma_0$ (to quickly fill the router’s queues when a message is generated). We have simulated both a $8 \times 8 \times 8$ (512 nodes) and a $16 \times 16 \times 16$ (4096 nodes) torus network, with the parameters reported in Table 1. The simulations have run in parallel on 160 threads on an Intel shared-memory system (Xeon CPU E7-8850, 8 processors, 10 cores/processor, 2 hyper-threads/core) with a GNU/Linux operating system, and have taken 40 hours to complete. For each single packet flowing in the network the following information has been tracked:

1. Number of traveled hops,
2. Lifetime from generation to consumption,
3. Whether and how derouted (WIDN vs OIDN).

4.1 Results

The improvement achieved by OFR against ABR in maximum throughput is quite remarkable, both for the $k = 8$ and $k = 16$ networks. The data reported in Table 2 for the $16 \times 16 \times 16$ network show that there is an increment in the maximum sustainable bandwidth, which goes from +14% for Uniform up to +114% for the extensively used Butterfly/FFT communication pattern.

Since the POR policy already exploits non-minimal links, the improvement against it is less conspicuous. However, our

Table 3: Ratio of derouted packets. OFR (OIDN and WIDN) vs. POR on a $16 \times 16 \times 16$ network.

Pattern	OFR/OIDN	OFR/WIDN	OFR (TOT)	POR
Butterfly/FFT	0.31	0.10	0.41	0.35
Transposition	0.04	0.10	0.14	0.10
3D Transposition	0.32	0.20	0.52	0.53
Uniform	0.06	0.12	0.18	0.13
Bit-Reverse	0.09	0.12	0.21	0.24

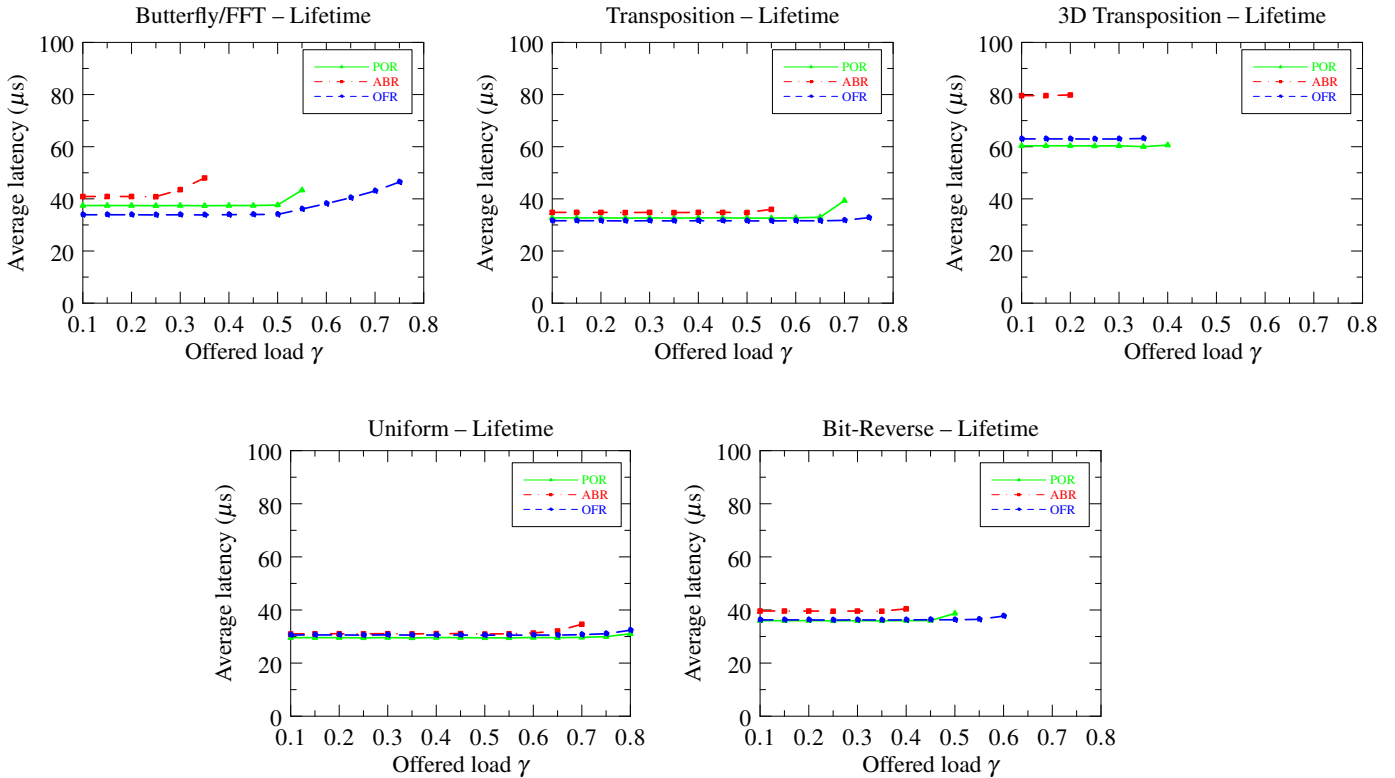


Figure 4: Simulation results: OFR vs. ABR vs. POR – Average packet lifetime, $16 \times 16 \times 16$ network. Latencies not shown (e.g., ABR one for Butterfly/FFT and $\gamma = 0.5$) are unbounded, the largest shown offered load for each pattern/routing policy is its maximum sustained throughput γ^* (e.g., for Butterfly/FFT and ABR, $\gamma^* = 0.35$). A summary of the maximum throughputs is given in Table 2, for both $k = 16$ and $k = 8$.

policy increases its perform as the size of the network increases. This is because the outflank derouting paths exploited by OFR come with a constant dilation of up to 6Δ ($= 12$ hops in our simulations) which is significant for small networks but becomes negligible as the average path length increases. Typical network size in top HPC systems [1] is some order of magnitude larger than the networks, so the benefits of adopting OFR in these systems are even stronger. We can see empirical evidence of the improvement in performance for larger sizes in our simulations. Comparing OFR against POR we see that for the smaller $8 \times 8 \times 8$ network the maximum sustainable bandwidth is quite similar, but POR wins over OFR in two cases, in one cases it loses and in two there is a draw. When moving to the larger $16 \times 16 \times 16$ network the situation is reversed: OFR wins in three cases, loses in one and there is one draw, registering an improvement against POR which is up to a +36% for the Butterfly/FFT pattern.

In Table 3 we show the ratio of packets which have been derouted both by the OFR and the POR algorithms. The values remain pretty stable within the range $\gamma \leq \gamma^*$ (see, e.g., Fig. 5). One might expect the ratio of derouted packets to be smaller at lower injection rates than at higher ones, but since the traffic is generated in messages each of 96 packets, the routers' queues are rapidly filled even when the injection rate is low.

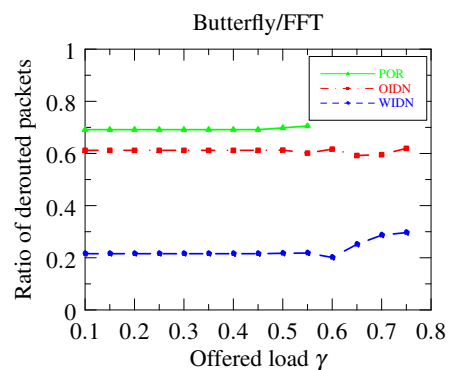


Figure 5: Ratio of derouted packets (OFR vs. POR) for the Butterfly/FFT pattern on a $16 \times 16 \times 16$ network.

5 Conclusions and future work

In this paper we have shown the potential of the OFR strategy, by exhibiting significant improvements on network performance for some realistic communication patterns. However, a few issues deserve further investigation:

- Before designing the hardware implementation of OFR, it would be interesting to strengthen its validation by testing the simulator on actual communication traces, rather than on synthetically generated ones.
- Although the profit function (15) adopted by OFR has proved to provide a good trade-off between congestion and path dilation, we would like to acquire a deeper understanding of the different effects of trading dilation for congestion, in order to theoretically justify the parameters and results obtained by empirical means.

Acknowledgment

We wish to express our gratitude to Fabio Schifano, for providing useful insights on the routing hardware and helping to discriminate implementable ideas from unimplementable ones. We would also like to thank Dirk Pleiter for pointing out some useful related work.

References

- [1] Top500 Supercomputer Sites, June 2013. <http://www.top500.org>.
- [2] ADIGA, N., BLUMRICH, M., CHEN, D., COTEUS, P., GARA, A., GIAMPAPA, M., HEIDELBERGER, P., SINGH, S., STEINMACHER-BUROW, B., TAKKEN, T., ET AL. Blue Gene/L torus interconnection network. *IBM Journal of Research and Development* 49, 2.3 (2005), 265–276.
- [3] AJIMA, Y., TAKAGI, Y., INOUE, T., HIRAMOTO, S., AND SHIMIZU, T. The Tofu interconnect. In *Hot Interconnects* (2011), pp. 87–94.
- [4] ALAM, S., BARRETT, R., BAST, M., FAHEY, M., KUEHN, J., MCCURDY, C., ROGERS, J., ROTH, P., SANKARAN, R., VETTER, J., ET AL. Early evaluation of IBM BlueGene/P. In *Proceedings of the 2008 ACM/IEEE conference on Supercomputing* (2008), IEEE Press, p. 23.
- [5] ANJAN, K. V., AND PINKSTON, T. M. Disha: a deadlock recovery scheme for fully adaptive routing. In *IPPS* (1995), pp. 537–543.
- [6] ARIMILLI, B., ARIMILLI, R., CHUNG, V., CLARK, S., DENZEL, W., DRERUP, B., HOEFLER, T., JOYNER, J., LEWIS, J., LI, J., NI, N., AND RAJAMONY, R. The percs high-performance interconnect. *High-Performance Interconnects, Symposium on 0* (2010), 75–82.
- [7] BEN-AROYA, I., CHINN, D. D., AND SCHUSTER, A. A lower bound for nearly minimal adaptive and hot potato algorithms. *Algorithmica* 21, 4 (1998), 347–376.
- [8] BILARDI, G., AND PREPARATA, F. P. Horizons of parallel computation. *J. Parallel Distrib. Comput.* 27, 2 (1995), 172–182.
- [9] BLUMRICH, M., CHEN, D., COTEUS, P., GARA, A., GIAMPAPA, M., HEIDELBERGER, P., SINGH, S., STEINMACHER-BUROW, B., TAKKEN, T., AND VRANAS, P. Design and analysis of the BlueGene/L torus interconnection network. *IBM Research Report RC23025 (W0312-022)* 3 (2003).
- [10] BORODIN, A., AND HOPCROFT, J. E. Routing, merging, and sorting on parallel models of computation. *J. Comput. Syst. Sci.* 30, 1 (1985), 130–145.
- [11] BROOKS, J., AND KIRSCHNER, G. Cray XT3 and Cray XT Series of supercomputers. In *Encyclopedia of Parallel Computing*. 2011, pp. 457–470.
- [12] BUSCH, C., MAGDON-ISMAIL, M., AND XI, J. Optimal oblivious path selection on the mesh. *IEEE Trans. Computers* 57, 5 (2008), 660–671.
- [13] CHEN, D., EISLEY, N. A., HEIDELBERGER, P., SENGER, R. M., SUGAWARA, Y., KUMAR, S., SALAPURA, V., SATTERFIELD, D. L., STEINMACHER-BUROW, B., AND PARKER, J. J. The IBM Blue Gene/Q interconnection network and message unit. In *Proceedings of 2011 International Conference for High Performance Computing, Networking, Storage and Analysis* (New York, NY, USA, 2011), SC '11, ACM, pp. 26:1–26:10.
- [14] CHINN, D. D., LEIGHTON, F. T., AND TOMPA, M. Minimal adaptive routing on the mesh with bounded queue size. *J. Parallel Distrib. Comput.* 34, 2 (1996), 154–170.
- [15] DALLY, W. J., AND SEITZ, C. L. Deadlock-free message routing in multiprocessor interconnection networks. Tech. Rep. 5206:TR:86, Computer Science Department, California Institute of Technology, 1985.
- [16] DALLY, W. J., AND SEITZ, C. L. Deadlock-free message routing in multiprocessor interconnection networks. *IEEE Trans. Computers* 36, 5 (1987), 547–553.
- [17] DALLY, W. J., AND TOWLES, B. Route packets, not wires: On-chip interconnection networks. In *DAC* (2001), pp. 684–689.
- [18] DUATO, J. A new theory of deadlock-free adaptive routing in wormhole networks. *IEEE Trans. Parallel Distrib. Syst.* 4, 12 (1993), 1320–1331.
- [19] DUATO, J. A necessary and sufficient condition for deadlock-free routing in cut-through and store-and-forward networks. *IEEE Trans. Parallel Distrib. Syst.* 7, 8 (1996), 841–854.

- [20] EL-MOURSRY, A., EL-MAHDY, A., AND EL-SHISHINY, H. An efficient in-place 3d transpose for multicore processors with software managed memory hierarchy. In *Proceedings of the 1st international forum on Next-generation multicore/manycore technologies* (New York, NY, USA, 2008), IFMT '08, ACM, pp. 10:1–10:6.
- [21] FOUNDATION, F. S. GNU Lesser General Public License. Version 3.
- [22] GEOFFRAY, P., AND HOEFLER, T. Adaptive routing strategies for modern high performance networks. In *Hot Interconnects* (2008), pp. 165–172.
- [23] KAKLAMANIS, C., KRIZANC, D., AND TSANTILAS, T. Tight bounds for oblivious routing in the hypercube. *Math. Systems Theory* 24, 4 (1991), 223–232.
- [24] KERMANI, P., AND KLEINROCK, L. Virtual cut-through: A new computer communication switching technique. *Computer Networks* 3 (1979), 267–286.
- [25] MARTÍNEZ-RUBIO, J. M., LÓPEZ, P., AND DUATO, J. Fc3d: Flow control-based distributed deadlock detection mechanism for true fully adaptive routing in wormhole networks. *IEEE Trans. Parallel Distrib. Syst.* 14, 8 (2003), 765–779.
- [26] PIVANTI, M., SCHIFANO, S. F., AND SIMMA, H. An fpga-based torus communication network. *PoS LATTICE2010* (2011).
- [27] PUENTE, V., BEIVIDE, R., GREGORIO, J. A., PRELLEZO, J. M., DUATO, J., AND IZU, C. Adaptive Bubble Router: A design to improve performance in torus networks. In *ICPP* (1999).
- [28] PUENTE, V., IZU, C., BEIVIDE, R., GREGORIO, J. A., VALLEJO, F., AND PRELLEZO, J. M. The Adaptive Bubble Router. *J. Parallel Distrib. Comput.* 61, 9 (2001), 1180–1208.
- [29] RÄCKE, H. Optimal hierarchical decompositions for congestion minimization in networks. In *STOC* (2008), pp. 255–264.
- [30] RÄCKE, H. Survey on oblivious routing strategies. In *CiE* (2009), pp. 419–429.
- [31] ROSCOE, A. Routing messages through networks: an exercise in deadlock avoidance. In *Proceedings of 7th occam User Group technical meeting, IOS BV, Amsterdam* (1987).
- [32] SCOTT, S., AND THORSON, G. The Cray T3E network: adaptive routing in a high performance 3D torus. In *Hot Interconnects IV* (1996), pp. 147–156.
- [33] SINGH, A., DALLY, W. J., GUPTA, A. K., AND TOWLES, B. GOAL: A load-balanced adaptive routing algorithm for torus networks. In *ISCA* (2003), IEEE Computer Society, pp. 194–205.
- [34] SINGH, A., DALLY, W. J., GUPTA, A. K., AND TOWLES, B. Adaptive channel queue routing on k-ary n-cubes. In *SPAA* (2004), P. B. Gibbons and M. Adler, Eds., ACM, pp. 11–19.
- [35] SINGH, A., DALLY, W. J., TOWLES, B., AND GUPTA, A. K. Locality-preserving randomized oblivious routing on torus networks. In *SPAA* (2002), pp. 9–13.
- [36] SINGH, A., DALLY, W. J., TOWLES, B., AND GUPTA, A. K. Globally adaptive load-balanced routing on tori. *Computer Architecture Letters* 3 (2004).
- [37] VALIANT, L. G. A scheme for fast parallel communication. *SIAM J. Comput.* 11, 2 (1982), 350–361.
- [38] VALIANT, L. G., AND BREBNER, G. J. Universal schemes for parallel communication. In *STOC '81* (New York, NY, USA, 1981), ACM, pp. 263–277.
- [39] VARGA, A. Omnet++. In *Modeling and Tools for Network Simulation*. 2010, pp. 35–59.
- [40] VÖCKING, B. Almost optimal permutation routing on hypercubes. In *STOC* (2001), pp. 530–539.